HiSST: 3rd International Conference on
High-Speed Vehicle Science Technology
14 -19 April 2024, Busan, Korea

Particle-based Simulation of Solid Rocket Plume at High Altitude

Yeongho Shin[1], Eunji Jun[2]

Abstract

Solid rocket motors (SRMs) are widely used in military and space missions due to their cost-effectiveness and compact design. However, the design optimization of SRMs poses unique challenges compared to liquid-propellant rockets. One primary concern is the emission of micron-sized alumina particles in the exhaust flow. These particles make up nearly 30% of the total mass flow, significantly affecting the flow properties. The exhaust flow with alumina particles can underexpand and backflow due to the rarefied atmosphere, posing potential risks such as base heating, erosion, and contamination. Understanding the exhaust flow dynamics can lead to more efficient SRM designs, potentially improving the efficiency and reducing operational risks. To simulate the multiscale gas flow with solid particles, this study employs two gas-solid interaction models to consider interphase dynamics. Burt's gas-solid interaction model is utilized for two-phase flow simulation. When Burt's assumption of negligibly small solid particle size breaks down in continuum gas regions, the Gas-Solid Synchronous (GSS) model is used to determine the gas-solid interactions. SRM exhaust flow conditions are based on prior studies, while the free-stream flow conditions are obtained from NRLMSISE-2.0 atmosphere model. The results present the impact of alumina particles on the plume and characteristics of backflowing gas around the SRM at 114km and 183km.

Keywords: Direct Simulation Monte Carlo (DSMC), Solid Rocket Motor (SRM) plume, two-phase flow

1. Introduction

Numerical simulation of solid rocket motor (SRM) plume at high altitudes has been studied in recent decades. The SRMs are widely used in military and space applications due to simplicity and cost-effectiveness. Despite their widespread use, SRMs pose significant engineering challenges, regarding the exhausts produced during their operation. During flight at high altitudes, high-density gas and agglomerated alumina particles in the combustion chamber are released into the nozzle. The exhausted solid particles are propelled and dispersed, while the gas flow undergoes acceleration and rapid expansion due to the rarefied atmosphere. The expanding gas flow transitions from continuum to rarefied regime, exhibiting non-equilibrium characteristics. This gas flow is considered as the multiscale flow as it covers the wide range of gas flow regimes. On the other hand, these micron-sized alumina particles make up nearly 30% of the total mass flow, considerably affecting the flow properties. The solid particles in the gas flow experience collision with gas molecules, resulting in mass, momentum, and energy transfer between the two phases. These interactions in the two-phase flow can cause complex phenomena such as phase change, wave propagation, and flow instabilities. For solid-solid interaction, it may affect the net flow depending on the types of flows. However, in this study, solid-solid interaction is not considered when the solid volume fraction is lower than 0.001 and the collision frequency of solid-solid interaction is much lower than that of gas-gas or gas-solid interactions. Thus, accurate modeling of both multiscale gas flow and gas-solid interactions is required to simulate the SRM plume at high altitudes.

The simulation of multiscale gas flow regimes requires the Boltzmann equation, which statistically

[1] *Graduate Student, Dept. of Aerospace Engineering, KAIST, South Korea*
[2] *Assistant Professor, Dept. of Aerospace Engineering, KAIST, South Korea, E-mail: eunji.jun@kaist.ac.kr*

represents the gas velocity distribution function. The solution to the Boltzmann equation can be approximated using the Direct Simulation Monte Carlo (DSMC) method, which involves tracking the movement and collision of computational gas molecules [1]. The DSMC method is applicable in a wide range of gas flow regimes where binary collision is dominant. To model gas-solid interaction in the DSMC framework, Gallis et al. first introduced a one-way coupled model based on the Maxwell-Lord Gas-Surface Interaction (GSI) model [2]. This one-way coupled model computes the force and heat transfer from monatomic gas molecules to a solid particle. Subsequently, Burt and Boyd extended Gallis' model to a two-way coupled model based on the Maxwell GSI model [3]. Burt's two-way coupled model accounts for the bi-directional interaction between polyatomic gas molecules and solid particles by reproducing the reflection of gas molecules on solid particle surfaces.

Burt's model is applicable to a broad range of two-phase flows under various assumptions. One of the assumptions is a negligibly small solid particle diameter, D, compared to the local gas mean free path, λ, so that the local gas flow around the solid particle is free-molecular. This assumption, however, tends to fail in high-density gas regions such near SRM nozzle where λ becomes small. Therefore, this paper presents the Gas-Solid Synchronous (GSS) model, an alternative gas-solid interaction model to compensate for the limitation on solid particle diameter compared to the local gas mean free path, λ. The GSS model consists of gas-to-solid and solid-to-gas models to account for the bi-directional interaction between the two phases. The GSS gas-to-solid model employs semi-empirical force and heat transfer models to consider complex physical mechanisms around a solid particle, while the GSS solid-to-gas model uses conservation laws to update velocities and rotational energies of gas molecules affected by solid particles. Then, a hybrid gas-solid interaction model built on Burt's and GSS models is used to simulate the SRM exhaust at high altitudes.

The rest of the paper is organized as follows: Section 2 presents methodologies for the gas-gas interaction. The GSS model is detailed in Section 3. The numerical method of the hybrid model based on the DSMC framework is described in Section 4. Section 5 validates the GSS model against Burt's model and investigates the characteristics of each gas-solid interaction models. The summary and future work for SRM plume simulation is provided in Section 6.

2. Gas-gas interaction

The gas-gas interaction is governed by the Boltzmann equation. Based on a statistical approach, the Boltzmann equation describes the motion of particles in terms of a velocity distribution function as they collide and move through space:

$$\frac{\partial}{\partial t}(nf) + \vec{c}\cdot\frac{\partial}{\partial \vec{r}}(nf) + \frac{\vec{F}}{m}\cdot\frac{\partial}{\partial \vec{u}}(nf) = \int_{-\infty}^{\infty}\int_{0}^{4\pi} n^2[f^* f_1^* - f f_1]c_r \sigma d\Omega d\vec{u}_1 \quad (1)$$

where $f(t,r,u)$ is the velocity distribution function, t is the time, r is the position, u is the velocity, n is the number density, F is the external force, m is the molecular mass, c_r is the relative speed between two colliding particles, σ is the differential cross-section, Ω is the deflection angle of particles due to the collision, and the asterisk in superscript denotes the post-collisional velocity distribution function. The left-hand side of the equation represents the evolution of the velocity distribution function by particle transport, while the right-hand side describes the change in the velocity distribution function due to binary collisions.

The DSMC method, proposed by G.A. Bird, has been a widely accepted numerical solver for the Boltzmann equation [1]. The DSMC method decouples the particle transport and the intermolecular collision on the left and right-hand sides of the Boltzmann equation, respectively. The DSMC method tracks computational gas molecules, where each molecule represents a large number of actual gas molecules. The computational gas molecules translate with constant velocity until they experience collisions. To reproduce intermolecular collisions, the DSMC method uses the no-time-counter (NTC) to select gas-gas collision pairs. When an elastic collision occurs, the Variable Soft Sphere (VSS) model is employed to account for temperature-dependent viscosity and self-diffusion coefficients. In the case of an inelastic collision, the Larsen-Borgnakke (LB) model is applied to redistribute the translational and rotational energy of gas molecules. The flowchart of the DSMC method is presented in Fig. 1. In this study, the SPARTA code, an open-source DSMC solver developed by Sandia National Laboratories, is used.

3. Gas-Solid Synchronous model for gas-solid interaction

Burt's kinetic-based approach is effective for rarefied gas flow with solid particles, where the local gas mean free path, λ, tends to be much larger than the solid particle diameter, D [3]. In the case of multiscale two-phase flow simulation, however, the assumption could break down in high-density gas regions where λ decreases. When the assumption fails, the local gas flow around a solid particle is not free-molecular, leading to inhomogeneous gas velocity distribution functions. The variation in gas velocity distribution functions can induce complex mechanisms such as compression and temperature slip around the particle. Since these mechanisms can affect gas-solid interaction significantly, an alternative approach is required to predict gas-solid interaction in the high-density gas regions.

3.1. GSS gas-to-solid interaction model

A spherical solid particle immersed in a gas flow experiences drag and lift. This study, however, focuses solely on drag, which is expected to be several orders of magnitude larger than lift. While lift can be significant in strong shear flows with large pressure gradients, it is anticipated to be much lower than drag in two-phase flows, particularly when solid particle diameters are smaller than 100 μm. The rotation of a solid particle is not considered due to its negligible impact on the flow. Additionally, the effect of unsteady inviscid force, which can be important in rapidly accelerating gas flows, is ignored because of the relatively low Reynolds number. Therefore, the force on a solid particle, F, that only includes drag is computed as

$$\vec{F}_{s,i} = \frac{1}{2}\rho_g\left(\vec{U}_g - \vec{u}_{s,i}\right)\left|\vec{U}_g - \vec{u}_{s,i}\right|\pi R_{s,i}^2 C_D \tag{2}$$

where gas density is represented by ρ_g, gas bulk velocity by $\vec{U}_g$, and drag coefficient by C_D. However, the most accurate model to predict C_D is not clear. To predict C_D in Eq. (2), various semi-empirical drag models that are valid in all local gas flow regimes are numerically investigated, and the most accurate drag model is selected as the GSS gas-to-solid force model. The accuracy of the five semi-empirical drag models is examined against DSMC results based on the root mean squared percentage errors (RMSPE). Since Singh's drag model presented the lowest RMSPE of 12.1%, Singh's model in Eq. (3) is selected as the GSS drag model. After the force on a solid particle is determined, the Euler method is used to update the velocity of the solid particle with sufficiently small time step size to obtain a converged solution.

$$C_D = \begin{cases} 0.272\Theta\left(1+\frac{9.4}{\sqrt{\widetilde{Re}}}\right)^2 \frac{f_{Kn,W_r}}{1+Br^{1.8}} + C_{D,FM}\frac{Br^{1.8}}{1+Br^{1.8}} & if\ Ma_\infty \le 1.0, \\ \left(C_1\left(1-\beta\frac{U_{pk}}{U_\infty}\right) + 0.272\Theta_{\mathrm{pk}}\left(1+\frac{9.4}{\sqrt{\widetilde{Re}_{pk}}}\right)^2\right)\frac{f_{Kn,W_r}}{1+Br^{1.8}} + C_{D,FM}\frac{Br^{1.8}}{1+Br^{1.8}} & if\ Ma_\infty > 1.0. \end{cases} \tag{3}$$

A spherical solid particle in a gas flow can experience three types of heat transfer: conduction, convection, and radiation. Conduction involves heat transfer through a medium caused by a temperature gradient, while convection is the heat transfer due to the bulk motion difference between the gas flow and a solid particle. Radiation is heat transfer through the emission of electromagnetic waves. To consider the heat transfer by the collision of gas molecules on solid particle surfaces, the GSS model considers both conduction and convection. In this study, radiation is not included due to its complexities.

According to previous studies, a widely used approach to predict the heat transfer rate on a solid particle in all local gas flow regimes, $\dot{Q}_{s,i}$, is to interpolate heat transfer rates in locally free-molecular and continuum regimes, $\dot{Q}_{FM,i}$ and $\dot{Q}_{CM,i}$ respectively. If local gas flow around a solid particle is free-molecular, the analytical heat transfer rate on a solid particle can be obtained as:

$$\dot{Q}_{FM,i} = \sum_{k=1}^{M_g}\tau_i m_{g,k} n_{g,k}\left(\frac{2k_B T_g}{m_{g,k}}\right)^{1.5}\pi R_{s,i}^2\left(k_1[s_{ik}] - \frac{T_{s,i}}{T_g}k_2[s_{ik}] + \frac{1}{4}\Lambda_k\left(1-\frac{T_{s,i}}{T_g}\right)k_2[s_{ik}]\right) \tag{4}$$

Here, k is the gas species index, M_g is the number of gas species, n is the number density, $s_{ik} = \left|\vec{U}_g - \vec{u}_{s,i}\right|\sqrt{m_{g,k}/2k_B T_g}$ is the molecular speed ratio of the solid particle, and $k_1[s]$ and $k_2[s]$ are subsidiary functions given by Gallis et al. Based on the Maxwell GSI model, Eq. (4) denotes the heat transfer rate by gas-solid collisions, including conduction and convection.

If local gas flow around a solid particle is continuum, a semi-empirical model can be used to predict the heat transfer rate on a solid particle as:

$$\dot{Q}_{CM,i} = \pi D_i \kappa_g (T_r - T_{s,i}) Nu \tag{5}$$

Here, D_i is the solid particle diameter, κ_g is the thermal conductivity of the gas, T_r is the recovery temperature, and Nu is the average Nusselt number. Since the Nusselt number of two denotes pure conductive heat transfer and larger Nusselt numbers indicate more convective heat transfer, this approach includes both conduction and convection. The accurate prediction of $\dot{Q}_{CM,i}$, however, is challenging due to complex physical mechanisms around a solid particle. To address the issue, various approaches have been proposed to determine T_r, κ_g, and Nu in Eq. (5). For instance, Wiskel et al. employed Whitaker's heat transfer model, but they evaluated κ_g at the solid particle surface temperature to modify Whitaker's model. It suggests that a potential heat transfer model can be made by using different approaches to calculate each parameter. Therefore, each combination of methods to determine T_r, κ_g, and Nu for the computation of $\dot{Q}_{CM,i}$ and the interpolation schemes used for predicting $\dot{Q}_{s,i}$ can be a heat transfer model. The accuracy of each heat transfer model is numerically investigated against 108 DSMC results and the three parameters, T_r, κ_g, and Nu predicts the heat transfer rate most accurately when they are computed as

$$T_r = T_g \left(1 + \sqrt{Pr}\frac{\gamma-1}{2} Ma_\infty^2\right), \tag{6}$$

$$\kappa_g = \kappa_g[T_g], \tag{7}$$

$$Nu = 2 + 0.34 Re^{0.2} \mathrm{Pr}^{0.333} + 0.24 Re^{0.7} \mathrm{Pr}^{0.333}. \tag{8}$$

After $\dot{Q}_{CM,i}$ is computed using Eq. (5), various interpolation schemes are examined to predict the heat transfer rate on a solid particle in all local gas flow regimes, $\dot{Q}_{s,i}$. The RMSPE of the most accurate methods to compute T_r, κ_g, Nu, and $\dot{Q}_{s,i}$ in Eq. (6), (7), (8), and (9) is 9.97% and other models with larger errors are not presented in this study for simplicity.

$$\dot{Q}_{s,i} = \frac{\dot{Q}_{FM,i}\dot{Q}_{CM,i}}{\dot{Q}_{FM,i}+\dot{Q}_{CM,i}} \tag{9}$$

3.2. GSS solid-to-gas interaction model

Burt's solid-to-gas interaction model utilizes kinetic approaches such as the modified NTC and reflection models because it assumes a locally free-molecular gas flow around a solid particle. When this assumption is not valid, gas velocity distribution functions around the solid particle become inhomogeneous, and modeling solid-to-gas interaction in a kinetic-based approach becomes challenging. Thus, Li, J. et al., Li, Y. et al., and Chinnappan et al. proposed alternative methods to consider solid-to-gas interaction [4-6]. Based on the principles of momentum and energy conservation, their models determine post-collisional velocities and rotational energies of gas molecules affected by solid particles. However, those models do not include the change in kinetic energy of solid particles affected by gas-solid interaction. Therefore, this study presents a more robust solid-to-gas interaction model to ensure both momentum and energy conservation.

Using momentum conservation, the post-collisional bulk gas velocity, $\vec{U}_g^{t+1}$, is computed to account for the interphase momentum transfer as:

$$\vec{U}_g^{t+1} = \vec{U}_g^{t} - \frac{F_{num,s}}{F_{num,g}} \frac{\sum_{i=1}^{N_s} m_{s,i}(\vec{u}_{s,i}^{t+1} - \vec{u}_{s,i}^{t})}{m_{g,total}} \tag{10}$$

Here, $\vec{U}_g^t$ is the pre-collisional bulk velocity of gas molecules, $m_{s,i}$ is the mass of a solid particle, and $m_{g,total}$ is the total mass of computational gas molecules in the cell.
Based on energy conservation, the change in thermal and rotational energy of computational gas molecules, $\Delta E = \Delta E_{th} + \Delta E_{rot}$, is derived as:

$$\Delta E = -\frac{1}{2} m_{g,total} \left|\vec{U}_g^{t+1} - \vec{U}_g^{t}\right|^2 - \frac{F_{num,s}}{F_{num,g}} \sum_{i=1}^{N_s} \left\{\frac{1}{2} m_{s,i} \left|\vec{u}_{s,i}^{t+1} - \vec{u}_{s,i}^{t}\right|^2 + \left(T_{s,i}^{t+1} - T_{s,i}^{t}\right) c_{ps,i} m_{s,i} \Delta t\right\} \tag{11}$$

Where ΔE_{th} and ΔE_{rot} are the change in thermal and rotational energy of gas molecules, respectively. The first term denotes the change in energy of gas molecules due to momentum transfer, while the

second term represents the change in total energy of solid particles. According to the equipartition theorem, the change in energy per degree of freedom should be constant. Thus, ΔE can be divided into thermal and rotational energy components as:

$$\Delta E_{th} = \frac{\sum_{j=1}^{Ng} 3}{\sum_{j=1}^{Ng}(3+\Lambda_j)} \Delta E \tag{12}$$

$$\Delta E_{rot} = \frac{\sum_{j=1}^{Ng} \Lambda_j}{\sum_{j=1}^{Ng}(3+\Lambda_j)} \Delta E \tag{13}$$

When the changes in the bulk velocity and thermal energy are known, the post-collisional velocity of individual gas molecules, $\vec{u}_{g,j}^{t+1}$, within a cell can be computed as

$$\vec{u}_{g,j}^{t+1} = \left(\vec{u}_{g,j}^{t} - \vec{U}_g^t\right) \cdot \phi + \vec{U}_g^{t+1} \tag{14}$$

Here, ϕ is the scaling factor for gas thermal velocities defined as

$$\phi = \sqrt{\frac{E_{th}+\Delta E_{th}}{E_{th}}} \tag{15}$$

and E_{th} is the pre-collisional thermal energy of computational gas molecules.
Note that Eq. 14 shifts the mean and variance of the Maxwell-Boltzmann gas velocity distribution function to account for the momentum and energy transfer. Finally, the rotational energy of each gas molecule is scaled to maintain the rotational energy distribution as

$$e_{rot,j}^{t+1} = e_{rot,j}^{t} \cdot \frac{\Delta E_{rot}+\sum_{j=1}^{Ng} e_{rot,j}^{t}}{\sum_{j=1}^{Ng} e_{rot,j}^{t}} \tag{16}$$

4. Numerical methodology

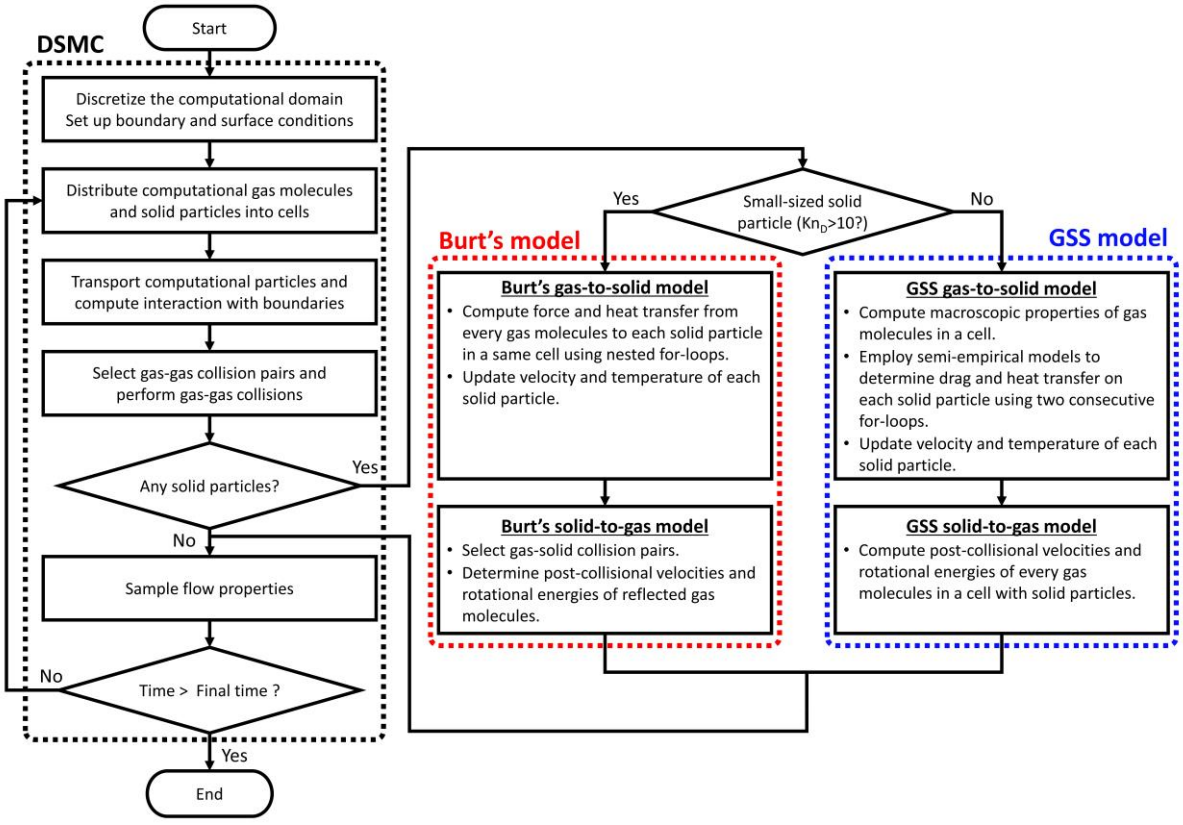

Fig. 1. A flowchart for multiscale two-phase flow simulation in the DSMC framework**.**

When gas flow with solid particles is simulated in SPARTA, computational particles including both gas and solid particles are deployed in the computational domain. The computational particles translate

with constant velocity until they collide. Then, two types of collisions, gas-gas and gas-solid, are considered to update velocities or internal energies of the computational particles. Until the SPARTA code reaches the final time, those processes are repeated to obtain properties of the two-phase flow.

If gas-solid collision occurs, either Burt's or GSS gas-to-solid models are used to calculate the force and heat transfer on solid particles. Subsequently, the velocities and temperatures of each solid particle are updated using the Euler methods. For solid-to-gas interaction, either Burt's or GSS model is employed to update the post-collisional velocities and rotational energies of computational gas molecules. Note that the hybrid gas-solid interaction model in Fig. 1 dynamically use either Burt's or GSS model based on applicable range of each model.

5. Result and Discussions

5.1. Solid rocket plume at high altitudes

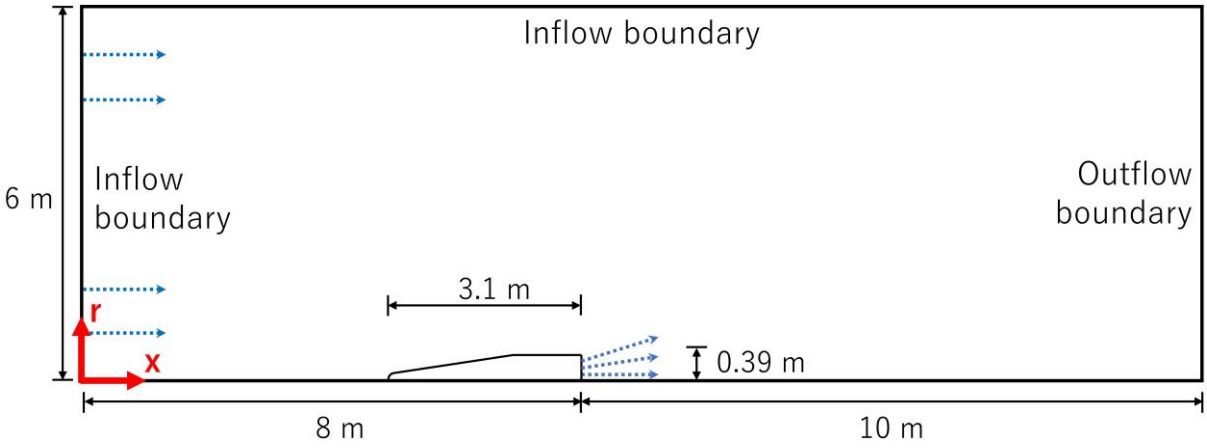

Fig. 2. The computational domain and boundary conditions of the SRM plume at high altitudes.

After the GSS model is validated in comparison with Burt's model, the hybrid gas-solid interaction model that includes Burt's and GSS models are used to simulate the solid rocket plume at the altitude of 114km and 183km [7]. The shape of the STAR-27 solid rocket and flow conditions of gas and solid particles are obtained from Burt, while free-stream gas flow conditions are obtained from NRLMSIS 2.0 [8]. The computational domain of the axisymmetric simulation is illustrated in Fig. 7. The nozzle exit radius is 0.39m and the shape of the solid rocket is approximated as a blunted cone-cylinder with the length of 3.1m. Similar to Burt's simulation, the solid rocket surface is assumed to be fully diffuse wall with the temperature of 300 K.

Table 2. Gas flow conditions of the SRM plume at the nozzle exit plane.

n_{H2} [m-3]	n_{N2} [m-3]	n_{CO} [m-3]	T_g [K]	U_g [m/s]
1.388×10^{23}	1.132×10^{23}	1.132×10^{23}	1433	3113

Table 3. Solid particle flow conditions of the SRM plume at the nozzle exit plane.

D [μm]	n_{Al2O3} [m-3]	T_s [K]	U_s [m/s]
0.3	2.638×10^{10}	1562	2992
0.4	9.042×10^{10}	1634	3051
0.6	9.799×10^{10}	1834	3023
1.0	9.579×10^{10}	2293	2973
2.0	4.823×10^{10}	1920	2855

4.0	2.117×10^{10}	2178	2674
6.0	1.658×10^{9}	2407	2472

Table 4. Free-stream gas flow conditions at the altitude of 114km and 183km from NRLMSIS-2.0.

Altitude	n_{N2} [m-3]	n_{O2} [m-3]	n_{O} [m-3]	T_g [K]	U_g [m/s]
114km	6.18×10^{17}	1.21×10^{17}	8.71×10^{16}	289	4590
183km	4.92×10^{15}	4.38×10^{14}	4.22×10^{15}	798	6100

The flow conditions of gas and solid particle in the SRM plume are presented in Table 2 and 3. The plume gas consists of N2, H2, and CO with mole fractions of 0.38, 0.31, and 0.31, respectively. At the nozzle exit plane, the gas flow has a speed of 3113 m/s, a temperature of 1433 K, and a density of 0.011 kg/m^3. When gas-gas collision occurs, the variable soft sphere (VSS) and Larsen- Borgnakke (LB) model are used. For solid particles, solid particle properties from Burt is used where the particles are divided into seven diameters ranging from 0.3 to 6 μm with distinct speed and temperatures. Since the computational domain does not include the area inside the nozzle, gas and solid particle properties are assumed to be uniform at the nozzle exit. However, for radial velocity, the bulk velocities of gas and solid particles are adjusted linearly so that the off-axis angle reaches the value of 17.2 degree at the nozzle lip because the nozzle divergence angle is the 17.2 degree. Note that chemical reactions are not considered in this study. To obtain the free-stream gas flow conditions, the average density of each species and temperature of ambient gas from the year of 2007 to 2017 is computed using NRLMSIS-2.0, as shown in Table 4. The velocities of the solid at 114km and 183km are set to be 4.59 km/s and 6.1 km/s [2, 9].

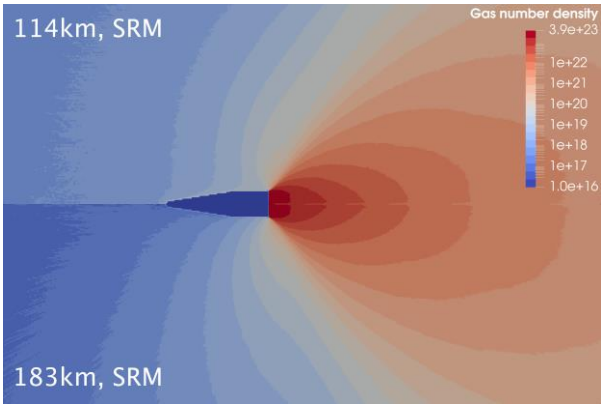

Fig. 3. The number density of gas and solid particles at the altitude of 114km and 183km.

Fig. 8 presents the contour of gas number density around the solid rocket at the altitude of 114km and 183km. The gas number densities at 114km and 183km show that the high-density gas exhausted at the nozzle exit rapidly expands toward the rarefied atmosphere and backflows. At the stagnation point, the gas number density normalized by free-stream gas number density is 11 and 19 at 114km and 183km, respectively. It shows that the gas flow in the plume tends to backflow more severely at 183km as expected.

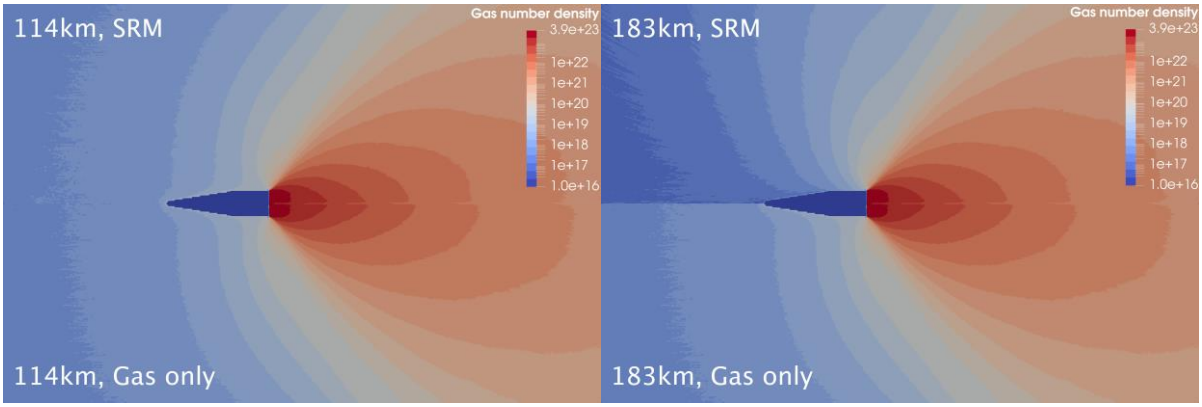

Fig. 4. The variation in gas number density at the altitude of 114km and 183km when solid particles are not included in the simulation.

Fig. 9 shows the influence of solid particles on the gas flow at 114km and 183km. At 114km, the result shows that solid particles have little impact on the number density of backflowing gas. However, at 183km, solid particles significantly affect the backflowing gas. Since solid particles are slower and hotter than gas flow, the gas flow with solid particles decelerates and heats up. The gas flow affected by solid particles tends to expand toward the radial direction, leading to relatively low gas number density around the solid rocket motor.

6. Conclusion

Burt's kinetic-based model is effective for predicting gas-solid interaction in a wide range of two-phase flows. However, in multiscale two-phase flows such as SRM plume at high altitudes, Burt's assumption of negligibly small solid particle diameter compared to the local gas mean free path ($Kn_D \gg 1$) could fail in high-density gas regions such as the SRM nozzle exit plane. Thus, this study proposes the GSS model to predict gas-solid interaction in continuum gas flow with no limitations on the solid particle size. Similar to Burt's model, the GSS model accounts for bi-directional interaction between gas and solid particles, including gas-to-solid and solid-to-gas interaction models. Then, the characteristics and limitations of Burt's and GSS models are evaluated. The result shows that Burt's model can capture gas-solid interaction regardless of the gas flow regimes, but Burt's model overestimates the interphase momentum and energy transfer when its assumption on Kn_D breaks down. On the other hand, the GSS model can predict gas-solid interaction accurately in continuum gas regions, while the GSS model cannot reproduce the interaction between the non-equilibrium gas flow and solid particles. Therefore, a hybrid gas-solid interaction model that includes both Burt's and GSS model is established to simulate the solid rocket motor (SRM) plume at 114 km and 183 km.

The result shows that the high-density gas exhausted at the nozzle exit rapidly expands toward the rarefied atmosphere and backflows. The gas flow tends to backflow more severely at 183km as expected. Alumina particles in the plume propelled at the nozzle exit are accelerated by gas flow at high-density gas regions near the nozzle. In the downstream, however, expanded and rarefied gas have little impact on solid particles, leading to simple dispersal of solid particles. For the impact of solid particles on backflowing gas, the result shows that solid particles barely affects backflowing gas at the altitude of 114 km. However, at 183km, the hot and slow solid particles make the gas flow decelerate and heat up, resulting in expansion of gas flow in the radial direction and low gas number density around the solid rocket. As a future work, additional physical models such as phase change of alumina particles and radiative heat transfer will be considered to simulate the SRM plume at high altitudes.

Acknowledgments

This research was supported by the Institute of Civil Military Technology Cooperation funded by the Defense Acquisition Program Administration and Ministry of Trade, Industry and Energy of Korean government under grant (No. 22-CM-EC-22) and the National Supercomputing Center with supercomputing resources including technical support (KSC-2022-CRE-0357).

References

1. Bird, G. A.: Molecular Gas Dynamics and the Direct Simulation of Gas Flows. Clarendon Press, (1994)
2. Gallis, M. A., Torczynski, J. R., and Rader, D. J.: An approach for simulating the transport of spherical particles in a rarefied gas flow via the direct simulation Monte Carlo method. Physics of Fluids 13(11), 3482–3492 (2001)
3. Burt, J.: Monte Carlo simulation of solid rocket exhaust plumes at high altitude. University of Michigan, (2006)
4. Li, J., Liu, Y., Wang, N., and Jin, L.: DSMC simulation of two-phase plume flow with UV radiation. AIP Conference Proceedings 1628(1), 569-580 (2014)
5. Li, Y., Ren, D., Bo, Z., Huang, W., Ye, Q., and Cui, Y.: Gas-particle two-way coupled method for simulating the interaction between a rocket plume and lunar dust. Acta Astronautica 157, 123-133 (2019)
6. Chinnappan, A. K., Kumar, R., and Arghode, V.: Modeling of dusty gas flows due to plume impingement on a lunar surface. Physics of Fluids 33, 053307 (2021)
7. Shin, Y., Kim, S., and Jun, E.: An approach for particle-based simulation of multiscale two-phase flows in the Direct Simulation Monte Carlo framework. Manuscript under review for Physics of Fluids.
8. Emmert, J. T., Drob, D. P., Picone, J. M., Siskind, D. E., Jones Jr., M., Mlynczak, M. G., Bernath, P. F., Chu, X., Doornbos, E., Funke, B., et al.: NRLMSIS 2.0: A whole-atmosphere empirical model of temperature and neutral species densities. Earth and Space Science 8(3), e2020EA001321 (2021)
9. Kinefuchi, K., Yamaguchi, H., Minami, M., Okita, K., and Abe, T.: In-flight S-band telemetry attenuation by ionized solid rocket motor plumes at high altitude. Acta Astronautica 165, 373–381 (2019)